Journal of Inflammation Research

Dovepress
open access to scientific and medical research

Open Access Full Text Article

ORIGINAL RESEARCH

Lymphatic Vessels in Chronic Rhinosinusitis

Vanessa-Vivien Pesold[1], Olaf Wendler[1], Franziska Gröhn[2], Sarina K Mueller[1]

[1]Department of Otolaryngology, Head and Neck Surgery, Friedrich-Alexander-Universität Erlangen-Nürnberg, Erlangen, BY, Germany; [2]Department of Chemistry and Pharmacy, Interdisciplinary Center for Molecular Materials, Friedrich-Alexander-Universität Erlangen-Nürnberg, Erlangen, BY, Germany

Correspondence: Sarina K Mueller, Friedrich-Alexander-Universität Erlangen-Nürnberg, Department of Otolaryngology, Head and Neck Surgery, Waldstrasse 1, Erlangen, 91054, Germany, Tel +49 91318533156, Fax +49 91318534749, Email mueller.sarinakatrin@gmail.com

Purpose: The purpose of this study was to analyze the nasal lymphatic system in order to uncover novel factors that might be involved in pathogenesis of chronic rhinosinusitis (CRS) with (CRSwNP) and without nasal polyps (CRSsNP).

Patients and Methods: Lymphatic vessels (LVs) and macrophages were localized and counted in the inferior and middle turbinate, the uncinate process and the ethmoid of CRSwNP and CRSsNP patients, the NP and the inferior turbinate of controls (n≥6 per group). Lysates of the same tissue types (n=7 per group) were analyzed for lymphatic vessel endothelial receptor 1 (LYVE-1), for matrix metalloproteinase 14 (MMP-14) and for Hyaluronic acid (HA) using ELISA. HA was localized in sections of CRSwNP NP, CRSsNP ethmoid and control inferior turbinate (n=6 per group). The results of HA levels were correlated to the number of macrophages in tissues. The nasal secretions of CRSwNP (n=28), CRSsNP (n=30), and control (n=30) patients were analyzed for LYVE-1 and HA using ELISA.

Results: The number of LVs was significantly lower in tissues of both CRS groups compared to the control. In the tissue lysates, LYVE-1 expression differed significantly between the CRSwNP tissues with a particularly high level in the NP. MMP-14 was significantly overexpressed in CRSwNP uncinate process. There were no significant differences in tissue HA expression. In the mucus LYVE-1 was significantly underexpressed in CRSsNP compared to CRSwNP and control, while HA was significantly underexpressed in both CRS groups. In the NP, HA and macrophages were accumulated particularly below the epithelium. Tissue levels of HA revealed a significant positive correlation with the number of macrophages.

Conclusion: CRS might be associated with an insufficient clearing of the nasal mucosa through the lymphatics. The accumulation of HA and macrophages might promote inflammation, fluid retention, and polyp formation. These results may provide novel CRS-associated factors.

Keywords: chronic rhinosinusitis, chronic rhinosinusitis with nasal polyps, mucus, inflammation, hyaluronic acid, lymphangiogenesis

Introduction

In inflammation, expansion of the lymphatic system (lymphangiogenesis) is crucial for providing a proper immune response and subsequently clearing extravasated fluid, pro-inflammatory mediators and cell debris, thus limiting edema formation and damage to the tissue. In the process, the LVs should reverse the effects of blood vessel expansion (angiogenesis), which occurs simultaneously with inflammation.

Consequently, an insufficient number of LVs in inflamed tissue may have serious consequences.

The hierarchical structure of the lymphatic vasculature begins with the lymphatic capillaries (LCs), which serve as the entry sites for the transported contents via their loose lymphatic endothelial cells (LECs). The LCs progress further into precollectors and collectors that are mainly responsible for transport. The receptor protein LYVE-1 is expressed by the LECs located at the initial ends of the LCs and plays an important role in generating effective immunological defense. The binding of antigen-presenting cells (APCs) to LYVE-1 via their HA glycocalyx results in diapedesis and, following antigen presentation in draining lymph nodes (dLNs), generation of the adaptive immune response.[1–4]

However, LYVE-1 can be shed by MMP-14, a zinc-dependent endopeptidase that has been shown to be highly active in chronically inflamed LVs. This process generates the soluble form of LYVE-1 (sLYVE-1), limiting the function of the membrane-bound protein and additionally inhibiting lymphangiogenesis.[5,6]

Received: 21 August 2023
Accepted: 30 November 2023
Published: 8 February 2024

As it is a major component of the extracellular matrix (ECM), HA plays an essential role in the tissue architecture and regulation of many cellular events due to its special water-binding capacity and its association with other ECM components. By accumulating and activating immune cells, it participates in inflammatory responses and remodeling processes in injured tissue. Physiologically, HA is partially degraded by uptake into the lymphatics via LYVE-1, where it is further decomposed in dLNs.[1,7–10] In contrast, accumulation of HA is associated with tumor growth and low immune responses.[11,12]

Insufficient lymphangiogenesis and impaired lymphatic function have already been observed in many diseases including inflammatory bowel disease and rheumatoid arthritis and are known to contribute to disease severity.[3] CRS is defined as an inflammation of the nasal mucosa lasting longer than three months. For a long time, different pathomechanisms were assumed to be responsible for the two phenotypes assigning them to specific endotypes.[13] However, recent findings in research point out that CRS may be a much more complex disease with many different factors contributing to its development.[14,15] Studies examining the contribution of the nasal microvasculature to CRS pathophysiology generally focus more on blood vessels than on LVs.[16] However, one study suggested that the occurrence of nasal polyps is connected to a lower lymphatic vessel density,[17] and currently there is also speculation about the participation of the micro lymphvasculature in non-type 2 inflammatory endotypes.[16]

Given these facts, taking a closer look at the nasal lymphatic structures and the possible consequences of an insufficient lymphatic disposal of the mucosa in the pathophysiological context of CRS may give further insight into the disease.

The sinuses cause the nasal mucosa to display a large surface area which primarily serves to warm up, humidify, and clean the inhaled air.[18] It has been shown that, even within a single sinus cavity, these numerous tissues can be affected to varying degrees by the endo- and phenotype present, which we wanted to consider.[19–21]

The objective of this study was, therefore, 1) to analyze the lymphatic system in order to identify novel factors that may play a role in the development of CRS and nasal polyposis and 2) to investigate how these factors vary in different anatomical subsites of the nasal mucosa in order to assume their association with inflammation and polyp formation.

Materials and Methods

Patients

This study was a prospective observational study approved by the institutional review board of the University of Erlangen-Nürnberg (No.: 17–269_1-B).

All patients provided written informed consent prior to participating. Demographic data were collected prospectively from these patients. The diagnosis of CRSwNP and CRSsNP was based on clinical diagnostic standards from the International Consensus Statement on Allergy and Rhinology.[22] The patients underwent surgery for either CRS (Functional Endoscopic Sinus Surgery, FESS, the removal of nasal polyps, septoplasty and turbinate reduction if necessary) or blockage of the nose (controls: septorhinoplasty and/or turbinate reduction). Exclusion criteria included ciliary dysfunction, autoimmune disease, cystic fibrosis, immunodeficiency, malignancies, gastroesophageal reflux disease, chronic rheumatic disease or any other disease requiring long-term (> 1 year) oral corticosteroid therapy. Additionally, patients who had used oral or topical corticosteroids or biologics three months prior to sample delivery were excluded. Thus, since corticosteroids and biologics can cause several adverse events[23,24] a falsification of the results due to their side effects was ruled out.

Mucus and Tissue Collection Technique

Mucus samples were taken from all patients by applying a compressed polyvinyl alcohol (PVA) sponge (Medtronic, Minneapolis, MN) to the nasal cavity adjacent to the middle turbinate for 5 minutes, taking care not to abrade the mucosa or contaminate the sponge with blood. For each patient, sponges of the same size were used and placed in the same region of the nasal mucosa to ensure reproducibility. For those patients undergoing surgery, tissue was collected using Blakesley forceps.

Mucus Extraction

To obtain mucus samples, liquid was extracted from the sponges by adding 400 µL phosphate-buffered saline (PBS, pH=8) with a Complete™ protease inhibitor cocktail (Roche Diagnostics GmbH, Germany). After 5 minutes the sponges

were centrifuged at 16,000 g for 5 minutes at 4°C. Afterwards this procedure was repeated once. Total protein was quantified using a bicinchoninic acid (BCA) Protein Assay Kit (Thermo Fisher Scientific, Bonn, Germany). All samples were aliquoted and stored at −80°C.This technique had been previously established by our group.[25]

Tissue Protein Extraction

For protein extraction the tissue was placed in a 350-µL solution of TPER Tissue Protein Extraction Reagent (Thermo Fisher Scientific, Bonn, Germany) and Inhibitor Cocktail (Carl Roth, Karlsruhe, Germany) and homogenized using the Ultra Turrax homogenizer (IKA®-Werke GmbH & CO. KG, Staufen, Germany). The resulting lysates were rotated for 2 hours at 4°C and then centrifuged at 10,000 g for 30 minutes at 4°C. The supernatant was collected and total protein was quantified using a bicinchoninic acid (BCA) Protein Assay Kit (Thermo Fisher Scientific, Bonn, Germany). All samples were aliquoted and stored at −80°C.

Analysis of Tissue and Mucus by Enzyme-Linked Immunosorbent Assay (ELISA)

ELISA tests of tissue samples were conducted for LYVE-1, MMP-14 and HA using lysates of CRSwNP inferior turbinate (iTN), CRSwNP middle turbinate (mTN), CRSwNP uncinate process (UP), CRSwNP ethmoid (ET), NP, CRSsNP iTN, CRSsNP mTN, CRSsNP UP, CRSsNP ET and control iTN (n=7 per group). ITN was the only tissue available for the control group since it is frequently removed in control patients undergoing septorhinoplasty. Additionally, ELISA tests of mucus samples were conducted for HA (CRSwNP n=28, CRSsNP n=31 and controls n=30) and LYVE-1 (CRSwNP n=28, CRSsNP n= 30 and controls n=30). All ELISAs were performed according to the manufacturer´s protocols.

For tissue LYVE-1, the tissue lysates were diluted 1:20 with Reagent Diluent (included in the kit), and the Human LYVE-1 DuoSet ELISA No. DY2089 (R&D Systems, Minneapolis, USA; assay range 31.2–2000 pg/mL) was used. For mucus LYVE-1, the nasal mucus was diluted 1:4 with Sample Diluent (included in the kit), and the LYVE-1 Human Uncoated ELISA Kit No. 88–52,239-22 (Thermo Fisher Scientific, Bonn, Germany; assay range 1.09–70 pg/mL) was used.

For MMP-14, the tissue lysates were diluted 1:2 with Reagent Diluent (included in the kit), and the Human Total MMP-14/MT1-MMP DuoSet ELISA No. DY918-05 (R&D Systems, Minneapolis, USA) was used.

For HA, the tissue lysates were diluted 1:150 and the nasal mucus was diluted 1:20 with Reagent Diluent (included in the kit), and the Human Hyaluronan DuoSet ELISA No. DY3614-05 (R&D Systems, Minneapolis, USA; assay range 0.4–90 ng/mL) was used.

Standard curves were generated and results were calculated by normalizing the values on the total protein concentration of the tissue and mucus samples. Values below the detection limit were excluded.

Tissue Analysis by Immunohistochemistry (IHC)

To localize the proteins of interest in the surgically collected tissue the ZytoChem-Plus AP Polymer-Kit (Zytomed Systems, Bargteheide, Germany) was used. To make the epitopes available for antibody binding, all sections underwent deparaffinization and heat-mediated antigen retrieval using either phosphate citrate buffer or Tris-EDTA buffer at 95°C for 20 minutes. Additional reduction in background staining was achieved by covering the sections with BLOXALL™ (Vector Laboratories, Inc.) for 10 minutes prior to a protein block with blocking solution (included in the kit). In order to localize MMP-14 and macrophages within the tissue sections, the antibodies mouse Anti-MMP-14 (R&D Systems, Bio-Techne, Wiesbaden, Germany) and mouse Anti-CD68 (macrophage marker protein;[26] Invitrogen, Karlsruhe, Germany) (see Additional Table 1 in additional data for detailed information) were incubated overnight at 4 °C. A nonspecific antibody (Cell Signaling Technology, Inc., Danvers, MA) served as negative control. Subsequently, the ZytoChem-Plus AP Reagent was applied. Antigens were stained with SIGMAFAST™ Fast Red TR/Naphthol AS-MX tablets (Sigma-Aldrich, Taufkirchen, Germany). Counterstaining was performed with Harris' hematoxylin solution (ORSAtec GmbH, Bobingen, Germany). The sections were covered with Aquatex (Merck, Darmstadt, Germany).

Tissue Analysis by Histochemistry

For HA staining by Astra blue, two sections per tissue were used. One section per tissue was first covered by hyaluronidase (Carl Roth, Karlsruhe, Germany) (4mg/ml in tris buffered saline (TBS)) at 37°C for 2 hours in order to obtain a control staining, since Astra blue targets all acid mucopolysaccharides.[27] All sections were then covered by a solution consisting of 4% Astra blue and 3% oxalic acid (both from Carl Roth, Karlsruhe, Germany) diluted in distilled water overnight at 60°C. After a brief acidification with 1% oxalic acid, counterstaining was performed with Nuclear Fast Red solution (Merck, Karlsruhe, Germany). The sections were drained from water using an ascending alcohol series and then covered in ROTI®Histokitt (Carl Roth, Karlsruhe, Germany).

For HA staining by the hyaluronic acid binding protein (HABP) which specifically targets hyaluronan,[28] two sections per tissue were used. One section per tissue was first covered by hyaluronidase (Carl Roth, Karlsruhe, Germany) (4 mg/mL in TBS) at 37°C for 2 hours in order to obtain a control staining. Background reduction was achieved by first covering all sections with BLOXALL™ for 10 minutes, followed by an avidin block for 15 minutes, followed by a biotin block, and finally followed by 1% horse serum (all from Vector Laboratories, Inc.) diluted in TBS for 20 minutes. HA was stained by covering the sections with HABP (Merck, Germany) diluted 1:150 in 0,2% horse serum in TBS overnight at 4°C. Afterwards, sections were covered by horseradish peroxidase-conjugated streptavidin (BioLegend GmbH, Koblenz, Germany) diluted 1:200 in TBS. Counterstaining was performed with Harris' hematoxylin solution. The sections were covered with Aquatex (Merck, Darmstadt, Germany).

Tissue Analysis by Immunofluorescence (IF)

IF was performed to co-stain LYVE-1 and podoplanin (PDPN) in the surgically collected tissue. To make the epitopes available for antibody binding, the paraffin sections underwent deparaffinization and heat-mediated antigen retrieval using either phosphate citrate buffer or Tris-EDTA buffer at 95°C for 20 minutes. Reduction in background staining was achieved by covering the sections with 1% Bovine Serum Albumin (BSA) in TBS for 20 minutes, and reduction of autofluorescence was achieved by covering the sections with TrueBlack® Lipofuscin Autofluorescence Quencher (Biotium, Fremont, USA) 1:40 diluted in TBS for 6 minutes. The primary antibodies rabbit anti-LVYE-1 (Abcam, Cambridge, UK) and rat anti-PDPN (Invitrogen, Karlsruhe, Germany) (see Additional Table 1 in additional data for detailed information) diluted in 0.1% BSA in TBS were incubated over night at 4 °C. Nonspecific antibodies (Cell Signaling Technology, Inc., Danvers, MA) served as negative controls. A negative control was performed for each tissue. Subsequently, the secondary antibodies Goat Anti-Rat IgG H&L (Cy3 ®) pre-adsorbed (polyclonal; Abcam, Cambridge, UK) and IgG (H+L) Goat anti-Rabbit, Alexa Fluor™ 488, Superclonal™ (polyclonal; Invitrogen, Karlsruhe, Germany) and 4′, 6-Diamidino-2-phenylindole dihydrochloride (DAPI) (Sigma-Aldrich, Taufkirchen, Germany), diluted to a final concentration of 0.1 µg/mL in 0.1% BSA in TBS, were incubated at room temperature for 1 hour. The sections were covered with Mowiol.[29]

Numerical Recording of Lymphatic Vessels and Macrophages in Tissue Sections

LYVE-1 and PDPN were co-stained using IF and the macrophage marker protein CD68[26] was stained using IHC in CRSwNP iTN (n=6), CRSwNP mTN (n=7), CRSwNP UP (n=7), CRSwNP ET (n=7), NP (n=8), CRSsNP iTN (n=7), CRSsNP mTN (n=7), CRSsNP UP (n=7), CRSsNP ET (n=7) and control iTN (n=13). The tissues for this analysis needed to be typical, as homogeneous as possible, similar in size and contain as few glands and bones as possible. The suitability of the tissues was checked previously by Hematoxylin and Eosin (H&E)[30] staining of the paraffin sections. After staining of the LVs and the macrophages, the whole tissue sections were photographed with a 4x objective lens using the BZ-9000 Fluorescence Microscope (Keyence Deutschland GmbH, Neu-Isenburg, Germany). Sections that did not fit in one frame were photographed in two parts. Then, counting analyses were carried out blinded and automated. The larger LVs expressing only PDPN were counted manually, while LVs whose LECs expressed both LYVE-1 and PDPN and macrophages were counted using ImageJ software.[31] For the LVs, by comparison to the negative control, an exposure threshold was initially set for each section. This exposure was then applied to the stained sections and the signals emerging from the background were detected. The size of the tissue was recorded using ImageJ software.[31] By calculating the captured area of one frame with a 4x objective lens, the

number of LVs and macrophages were accordingly normalized to an area of 7 mm^2. For larger tissues that needed to be photographed using two frames, the mean value was calculated.

Statistical Analysis

For demographic data, the p-value of age was calculated using the ordinary one-way ANOVA. For the results of gender, race and comorbidity, the Chi-square test was used. The results of the semiquantitative analysis of ELISA and the numerical recording of LVs and macrophages in tissues were calculated using the ordinary one-way ANOVA test. Groups were compared with each other using the Tukey's multiple comparisons test. Mean value and standard deviation were calculated for each group. For groups displaying statistically significant differences, the fold changes were calculated by dividing the mean values. All results were calculated using Prism (GraphPad Prism 9.2.0; GraphPad Software, La Jolla, CA). The same software was used for correlation analysis of HA and macrophages by Pearson's correlation. A false discovery rate cutoff of P <0.05 was used to detect significant differences between the groups. For the mucus samples, values exceeding the mean value plus three times the standard deviation were identified as outliers and excluded.

Results

Demographics

Demographic data is shown in Table 1. The table presents all patients included in this study. For the individual analyses, we selected our samples from these patient pools. Demographic data for the different experiments (ELISA, IHC, IF) are displayed in Additional Tables 2a–c) of the additional data. There were no significant differences between the CRSwNP, CRSsNP, and control groups (CRSwNP n=55, CRSsNP n=46 and control n=51) with respect to gender, race and allergic rhinitis. In both CRS groups, the patients' age was significantly higher compared to that of the control patients (p<0.0001). Comorbid asthma occurred significantly more often in CRSwNP (p=0.0004). The number of patients suffering from AERD was significantly higher in CRSwNP (p=0.0008). Moreover, there were significantly more smokers in the control group (p=0.0203).

Figure 1 shows a flow chart of the patients who were used for this study.

Table 1 Demographics of CRSwNP, CRSsNP and control patients in total. See Additional Tables 2a–c) of the additional data for demographic results of the patients used for the individual analyses. In some cases, not all data were available for one patient.

Characteristics in (%)	CRSwNP (n=55)	CRSsNP (n=46)	Control (n=51)	p-value
Age (years), mean ± SD	47.9±13.8	45.6±16.4	32.2±11.5	****(p<0.0001)
Gender				
Male	38/55 (69.1)	24/46 (52.2)	32/51 (62.7)	ns (p=0.2161)
Female	17/55 (30.9)	22/46 (47.8)	19/51 (37.3)	ns (p=0.2161)
Race				
Caucasian	55/55 (100)	46/46 (100)	51/51 (100)	Not applicable
Comorbidity				
Asthma	13/53 (24.5)	4/44 (9.1)	0/51 (0)	***(p=0.0004)
Environmental allergy	27/53 (50.9)	21/43 (48.8)	17/51 (33.3)	ns (p=0.1501)
AERD	7/53 (13.2)	0/43 (0)	0/51 (0)	***(p=0.0008)
Smoker	10/36 (27.8)	6/35 (17.1)	19/41 (46.3)	*(p=0.0203)

Notes: Asterisks indicate statistically significant results. *<0.05, ***<0.001, ****<0.0001.
Abbreviations: CRSwNP, chronic rhinosinusitis with nasal polyps; CRSsNP, chronic rhinosinusitis without nasal polyps; AERD, aspirin-exacerbated respiratory disease; SD, standard deviation; ns, not significant.

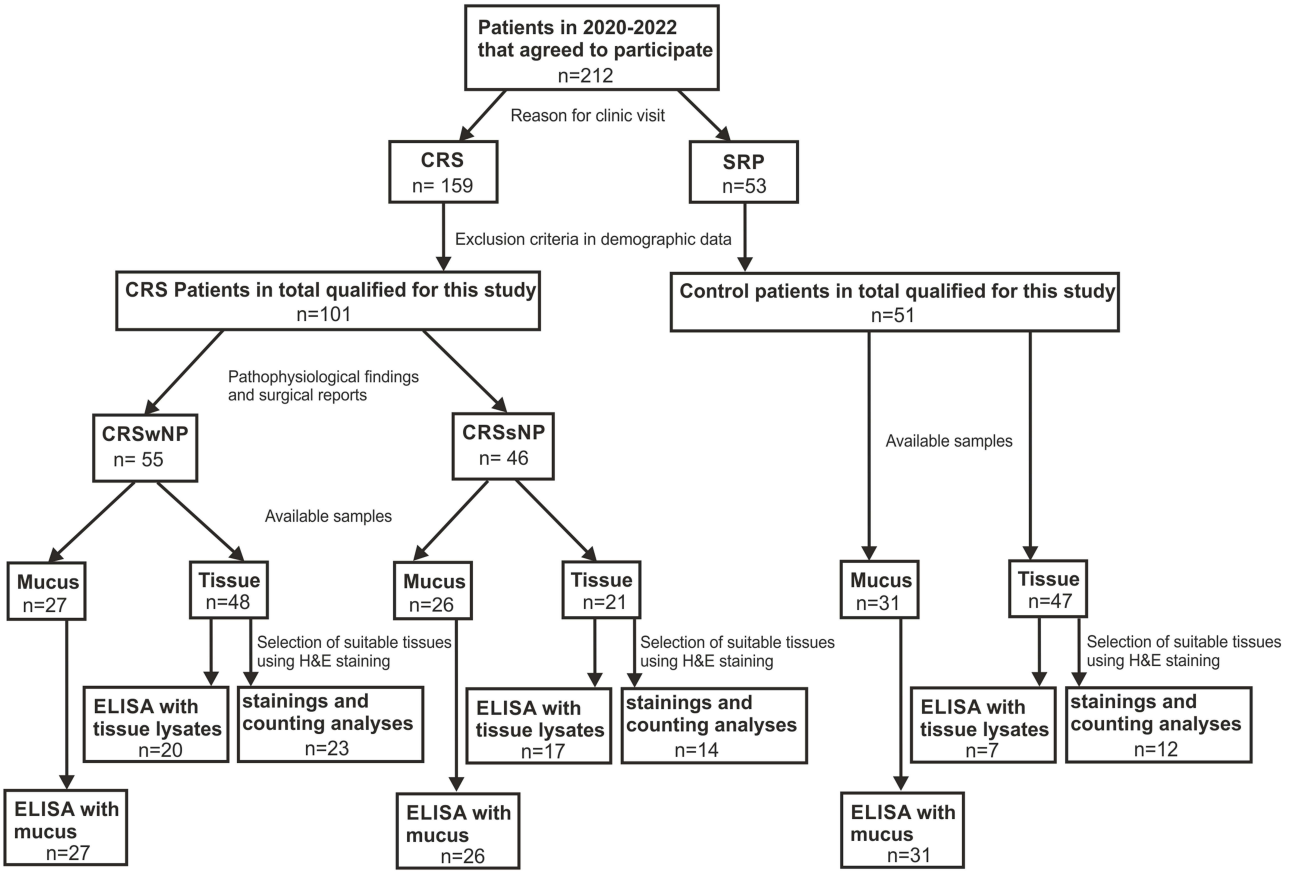

Figure 1 Flow chart of CRSwNP, CRSsNP and control patients used for this study.
Abbreviations: CRSwNP, chronic rhinosinusitis with nasal polyps; CRSsNP, chronic rhinosinusitis without nasal polyps; SRP, septorhinoplasty; H&E, Hematoxylin and Eosin.

Localization and Quantitative Analysis of LVs in CRSwNP, CRSsNP and Control Patients Using if

IF was performed for co-staining of LYVE-1 and PDPN in CRSwNP iTN (n=6), CRSwNP mTN (n=7), CRSwNP UP (n=7), CRSwNP ET (n=7), NP (n=8), CRSsNP iTN (n=7), CRSsNP mTN (n=7), CRSsNP UP (n=7), CRSsNP ET (n=7), and control iTN (n=13). Subsequently, LVs were counted and normalized to a tissue area of 7 mm^2. In each case, the whole tissue was considered.

LYVE-1 and PDPN are proteins expressed by LECs and therefore serve as frequent markers of LVs.[32,33] However, while PDPN is expressed by virtually all LECs,[34] LYVE-1 is only expressed by the endothelium located at the blind ends of the LCs. Consequently, LVs were differentiated into LVs expressing only PDPN but no LYVE-1 and possessing a larger lumen (=(pre-)collector vessels) and LVs expressing both PDPN and LYVE-1 and possessing a small lumen (=LCs), as previously described in the literature.[1,32,33,35] Examples of the IF stainings are shown in Figure 2a).

LYVE-1^-/ PDPN $^+$ LVs were almost exclusively found at the edge of the tissues directly under the epithelium (arrowheads). In contrast, LYVE-1^+/ PDPN $^+$ LVs were mostly located in the deeper layers of the stroma (arrows).

Mean values of LVs for each individual tissue type are displayed in Figure 2b).

LVs showed a heterogenous distribution pattern between the analyzed tissues. However, with the exception of the CRSwNP iTN, counting revealed fewer LVs of both types in all CRSwNP and CRSsNP tissues than in control iTN.

The results of statistical evaluation after summarizing all available tissues of the same CRS phenotypes (CRSwNP n=35, CRSsNP n=28, and control n=13) are displayed in Figure 2c and d). There, the results of the Tukey's multiple comparisons tests are displayed. The ANOVA summaries are displayed in Additional Table 3 of the additional data.

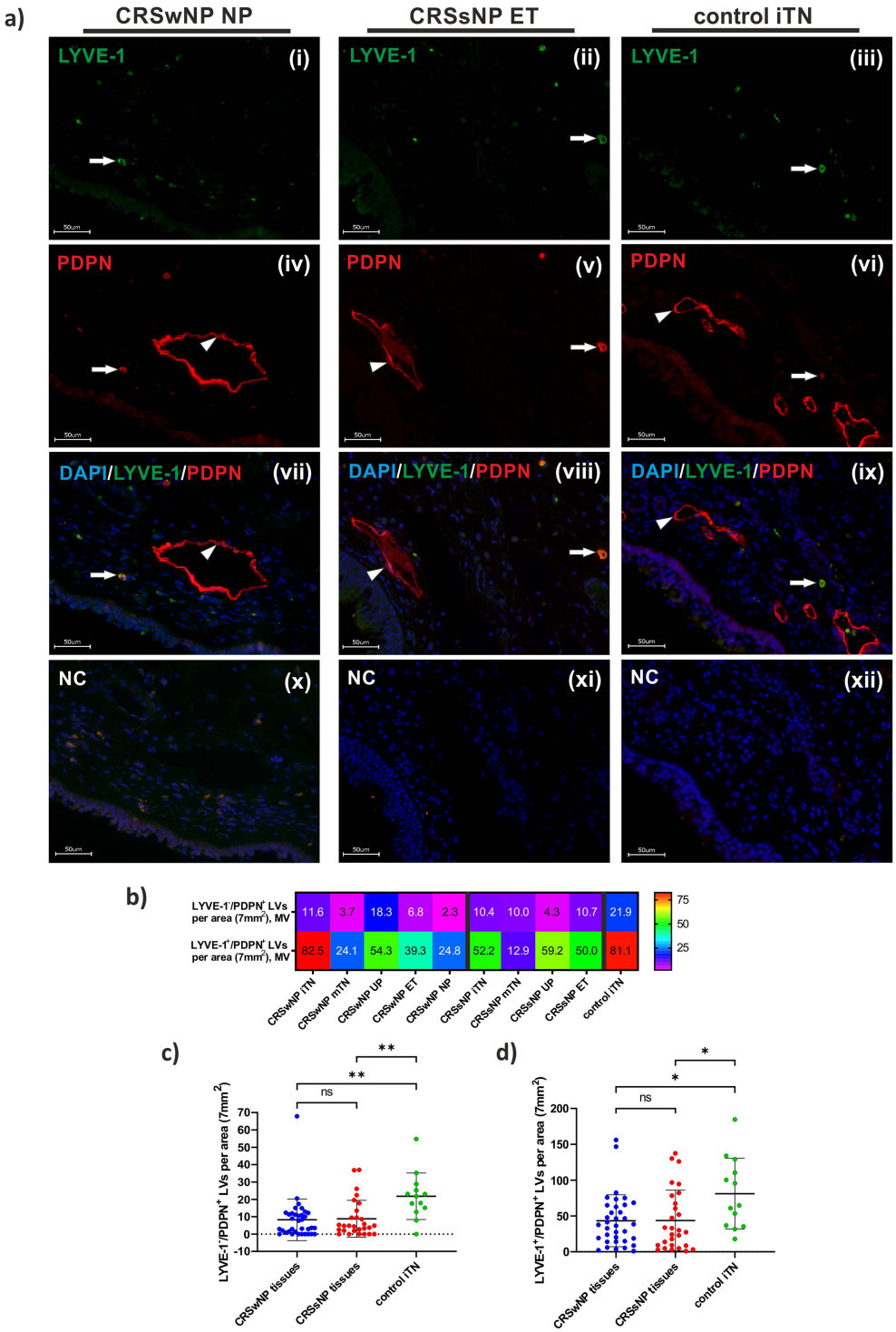

Figure 2 Immunofluorescence (**a**) of LYVE-1 (green) (panels (i), (ii) and (iii)) and PDPN (red) (panels (iv), (v) and (vi)) in CRSwNP, CRSsNP and control tissues (photographed with a 40x objective lens). The panels (vii), (viii) and (ix)) show the merged images. Staining of the nuclei was performed with DAPI (blue). Larger LVs located near the epithelium contain a visible lumen and their LECs express PDPN, but not LYVE-1 (arrowheads). Narrow initial ends of lymphatic capillaries are mostly located in the inner stroma, and their LECs expressed both proteins PDPN and LYVE-1 (arrows). Nonspecific antibodies served as negative controls (panels (x), (xi) and (xii)). The heat map (**b**) shows the mean values of the LV count in different tissues of CRSwNP, CRSsNP, and control patients normalized to an area of 7 mm^2. Scatter dot plots (**c** and **d**) including mean and SD error bars show the results of counting LVs in the different tissue types of CRSwNP (blue), CRSsNP (red), and control (green) patients normalized to an area of 7 mm^2. For (**c**) LYVE-1^- / PDPN $^+$ LVs statistically significant differences can be seen for CRSsNP vs control ($p<0.01$) and for CRSwNP vs control ($p<0.01$). For (d) LYVE-1^+/ PDPN $^+$ LVs statistically significant differences can be seen for CRSsNP vs control ($p<0.05$) and for CRSwNP vs control ($p<0.05$). Asterisks indicate statistically significant results. *<0.05, **<0.01.

Abbreviations: CRSwNP, chronic rhinosinusitis with nasal polyps; CRSsNP, chronic rhinosinusitis without nasal polyps; LYVE-1, lymphatic vessel endothelial receptor 1; PDPN, podoplanin; DAPI: 4',6-Diamidino-2-phenylindol; NC, negative control; LVs, lymphatic vessels; LECs, lymphatic endothelial cells; MV, mean value; iTN: inferior turbinate; mTN: middle turbinate; UP, uncinate process; ET, ethmoid; NP, nasal polyp; vs, versus; ns, not significant; SD, standard deviation.

LYVE-1^{-}/PDPN $^{+}$ LVs (Figure 2c) were significantly underexpressed in the tissues of CRSsNP (FC=0.4, p=0.0044) and CRSwNP (FC=0.38, p=0.0020) compared to control iTN, while comparison of CRSsNP and CRSwNP was not significant (p=0.9796).

LYVE-1^{+}/ PDPN $^{+}$ LVs (Figure 2d) were significantly underexpressed in the tissues of CRSsNP (FC=0.54, p=0.0214) and CRSwNP (FC=0.53, p=0.0159) compared to control iTN, while comparison of CRSsNP and CRSwNP was not significant (p=0.9996).

In general, inflamed and polypous nasal tissues contained fewer LVs compared to the control iTN (Figure 2).

Quantitative Analysis of LYVE-1 in CRSwNP, CRSsNP, and Control Patients Using ELISA

ELISAs for LYVE-1 were performed using tissue lysates of the iTN, mTN, UP, and ET from CRSwNP and CRSsNP patients, the NP from CRSwNP patients and the iTN from control patients (n=7 per group) and using the mucus samples of CRSwNP (n=28), CRSsNP (n=30), and control (n=30) patients. The results of the Tukey's multiple comparisons tests are displayed in the Figure 3a and b). The ANOVA summaries are displayed in Additional Table 3 of the additional data.

ELISA of tissue lysates (Figure 3a) revealed a significant overexpression of LYVE-1 in CRSwNP NP compared to CRSwNP iTN (FC=3.49, p<0.0001) within the CRSwNP tissues, while there were no significant results between the CRSsNP tissues. CRSwNP NP showed a significant overexpression compared to control iTN (FC=2.76, p<0.0001). Results revealed a continuous rise in LYVE-1 levels between the CRSwNP tissues mTN<UP<ET<NP.

ELISA of mucus (Figure 3b) revealed a significant underexpression of LYVE-1 in CRSsNP compared to the controls (FC=0.53, p=0.0151) and to CRSwNP (FC=0.052, p=0.0168), while comparison of CRSwNP and the controls was not significant (p>0.9999) (Figure 3).

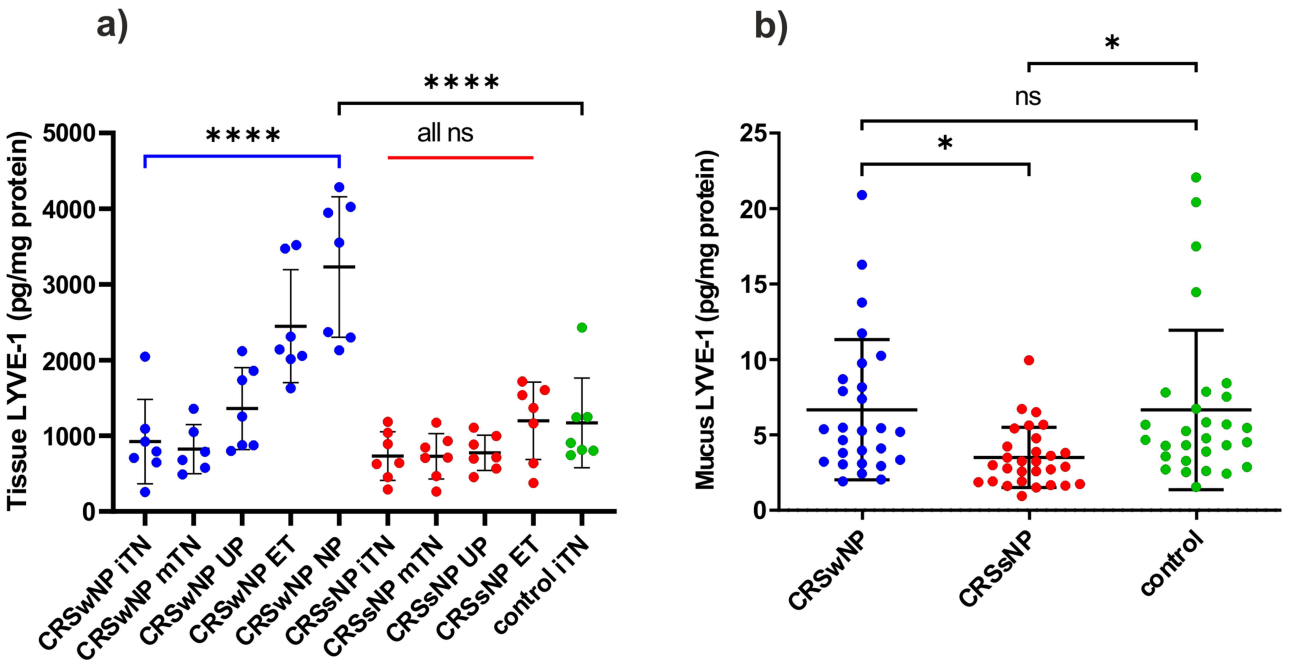

Figure 3 The scatter dot plot (**a**) including mean and SD error bars shows results of the quantitative analysis of LYVE-1 by ELISA in the tissue lysates (1 value below detection limit) of CRSwNP (blue), CRSsNP (red), and control (green) patients normalized to a total protein concentration. Significant differences can be seen for CRSwNP NP vs CRSwNP iTN (p<0.0001) and for CRSwNP NP vs control iTN (p<0.0001). The scatter dot plot (**b**) including mean and SD error bars shows results of the quantitative analysis of LYVE-1 by ELISA (3 outliers, no value below detection limit) in the nasal mucus of CRSwNP (blue), CRSsNP (red), and control (green) patients normalized to a total protein concentration. Outliers are not included. Statistically significant differences can be seen for CRSwNP vs CRSsNP (p<0.05) and for CRSsNP vs the controls (p<0.05). Asterisks indicate statistically significant results. *<0.05, ****<0.0001.

Abbreviations: CRSwNP, chronic rhinosinusitis with nasal polyps; CRSsNP, chronic rhinosinusitis without nasal polyps; iTN, inferior turbinate; mTN, middle turbinate; UP, uncinate process; ET, ethmoid; NP, nasal polyp; LYVE-1, lymphatic vessel endothelial receptor 1; ns, not significant; SD, standard deviation.

Quantitative Analysis and Localization of MMP-14 in CRSwNP, CRSsNP, and Control Patients Using ELISA and Histochemical Staining

ELISAs for MMP-14 were performed using tissue lysates of the iTN, mTN, UP, and ET from CRSwNP and CRSsNP patients, the NP from CRSwNP patients and the iTN from control patients (n=7 per group). IHC was performed to localize MMP-14 in the same tissue types. The result of the Tukey's multiple comparisons test is displayed in Figure 4a). The ANOVA summary is displayed in Additional Table 3 of the additional data.

Results of tissue MMP-14 (Figure 4a) revealed a significant overexpression of MMP-14 in CRSwNP UP compared to CRSwNP iTN (FC=2.02, p=0.0002) within the CRSwNP tissues, while there were no significant results between the CRSsNP tissues. CRSwNP UP showed a significant overexpression compared to control iTN (FC=2.08, p=0.0002).

Examples of IHC of MMP-14 in different tissue types are shown in the panels (i), (ii) and (iii) of Figure 4b). IHC results verified the results of ELISA. MMP-14 was expressed by epithelial cells as well as many other cell types within the whole stroma.

Quantitative Analysis and Localization of HA and Macrophages in CRSwNP, CRSsNP and Control Patients Using ELISA and Histochemical Staining

ELISAs for HA were performed using tissue lysates of the iTN, mTN, UP, and the ET from CRSwNP and CRSsNP patients, the NP from CRSwNP patients and the iTN from control patients (n=7 per group) and using the mucus samples of CRSwNP (n=28), CRSsNP (n=31), and control (n=30) patients. The results of the Tukey's multiple comparisons tests are displayed in the Figure 5a–c). The ANOVA summaries are displayed in Additional Table 3 of the additional data.

ELISA of the tissue lysates (Figure 5a) revealed no significant differences in HA expression either between different anatomical regions or between CRSwNP, CRSsNP, and controls.

ELISA of the mucus (Figure 5b) revealed a significant underexpression of HA in CRSsNP (FC=0.78, p=0.0362) and in CRSwNP (FC=0.66, p=0.0008) compared to the controls. Comparison of the mucus HA between CRSsNP and CRSwNP was not significant (p=0.3684).

Histochemical staining was performed for localizing HA in tissues of CRSwNP, CRSsNP and control patients. Examples are displayed in Figure 5e) (panels (i), (ii), (iii), (iv), (v), (vi), (vii) and (viii)). In order to verify the results shown that were obtained by Astra blue staining, sections of the same tissue were additionally stained with HABP (data not shown). Staining results showed that HA was present in the epithelial cell layers (blue arrows) of all sections. There were no visible quantitative differences in the presence of HA between the whole tissue slides. However, in NP hyaluronan was excessively located in the outer stroma directly under the epithelium, while it was located to a lesser extent in the inner stroma. In contrast, staining of CRSsNP ET and control iTN revealed the inner stroma and the glandular bundles contained therein as its main locations (blue arrowheads). In CRSwNP ET HA was detected throughout the whole tissue section. Mucopolysaccharides other than HA were found in the outer epithelial layers (pink arrows).

IHC was performed for macrophages in CRSwNP iTN (n=6), CRSwNP mTN (n=7), CRSwNP UP (n=7), CRSwNP ET (n=7), NP (n=8), CRSsNP iTN (n=7), CRSsNP mTN (n=7), CRSsNP UP (n=7), CRSsNP ET (n=7) and control iTN (n=13). Examples are shown in Figure 5e) (panels (ix), (x), (xi) and (xii)). Macrophages were detected in the outer stroma and throughout the whole epithelium. Subsequently, the macrophages were counted and normalized to a tissue area of 7 mm^2. In each case, the whole tissue slide was considered. Counting of macrophages (Figure 5c) revealed no significant differences either between different anatomical regions or between CRSwNP, CRSsNP, and controls.

Correlation analysis was performed using all tissues for which ELISA result of HA in lysate and number of macrophages were available (CRSwNP iTN (n=2), CRSwNP mTN (n=5), CRSwNP UP (n=4), CRSwNP ET (n=4), NP (n=5), CRSsNP iTN (n=4), CRSsNP mTN (n=2), CRSsNP UP (n=5), CRSsNP ET (n=1) and control iTN (n=1)). For correlation between HA and macrophages (Figure 5d), results revealed a weakly significant positive correlation (r=0.3807, p=0.0289).

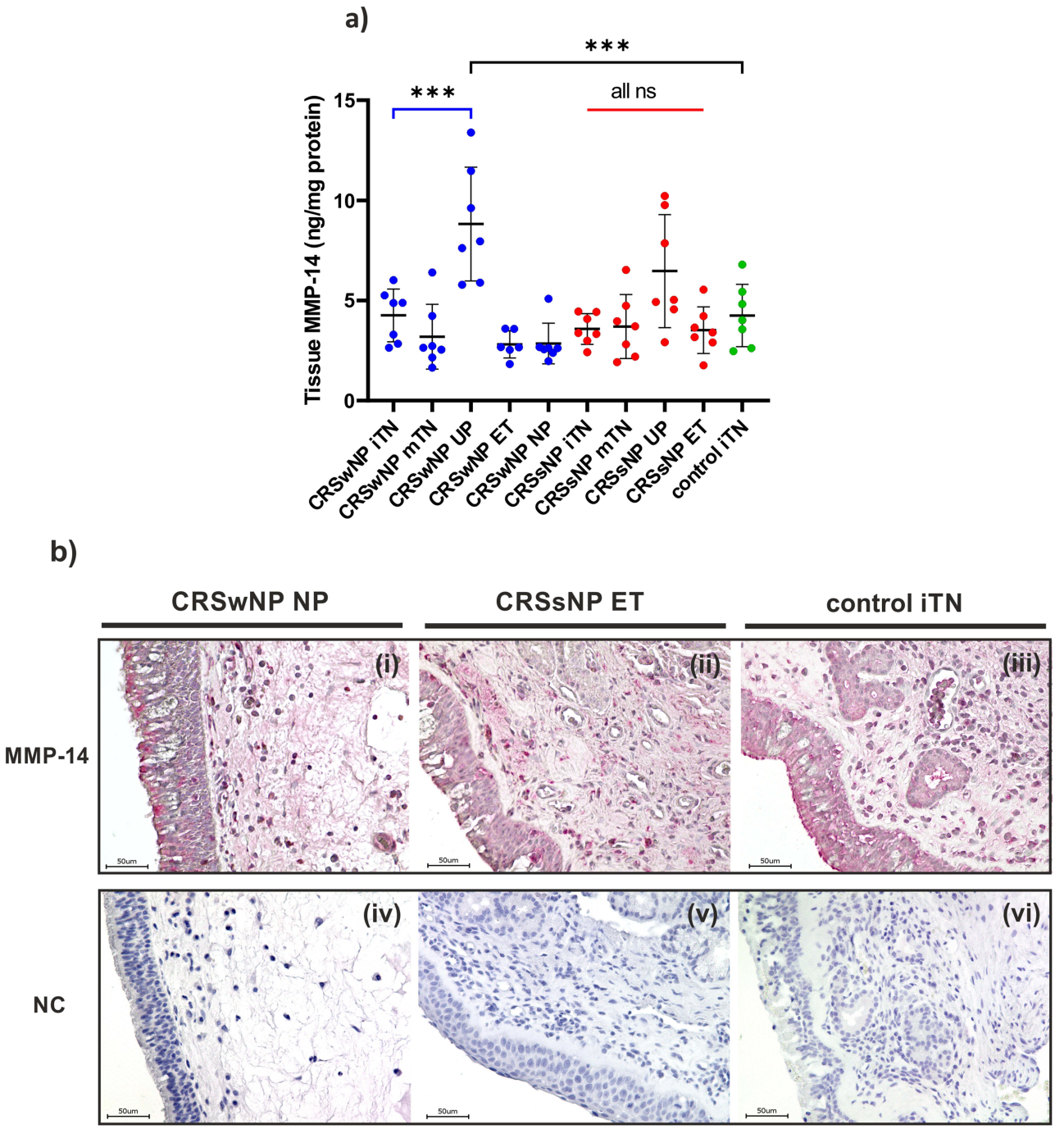

Figure 4 The scatter dot plot (**a**) including mean and SD error bars shows the results of the quantitative analysis of MMP-14 by ELISA in the tissue lysates (1 value below detection limit) of CRSwNP (blue), CRSsNP (red), and control (green) patients normalized to a total protein concentration. Significant differences can be seen for CRSwNP UP vs CRSwNP iTN ($p<0.001$) and for CRSwNP UP vs control iTN ($p<0.001$). Immunohistochemistry (**b**) of MMP-14 (panels (i), (ii) and (iii)) in CRSwNP, CRSsNP, and control tissues (photographed with a 40x objective lens). The NCs are displayed in the panels (iv), (v) and (vi). Antigens were stained with Red Alkaline Phosphatase-Substrate, and counterstaining was performed with Harris' hematoxylin solution. Asterisks indicate statistically significant results. ***<0.0001.

Abbreviations: CRSwNP, chronic rhinosinusitis with nasal polyps; CRSsNP, chronic rhinosinusitis without nasal polyps; MMP-14, matrix metalloproteinase 14; iTN, inferior turbinate; mTN, middle turbinate; UP, uncinate process; ET, ethmoid; NP, nasal polyp; ns, not significant; NC, negative control; SD, standard deviation.

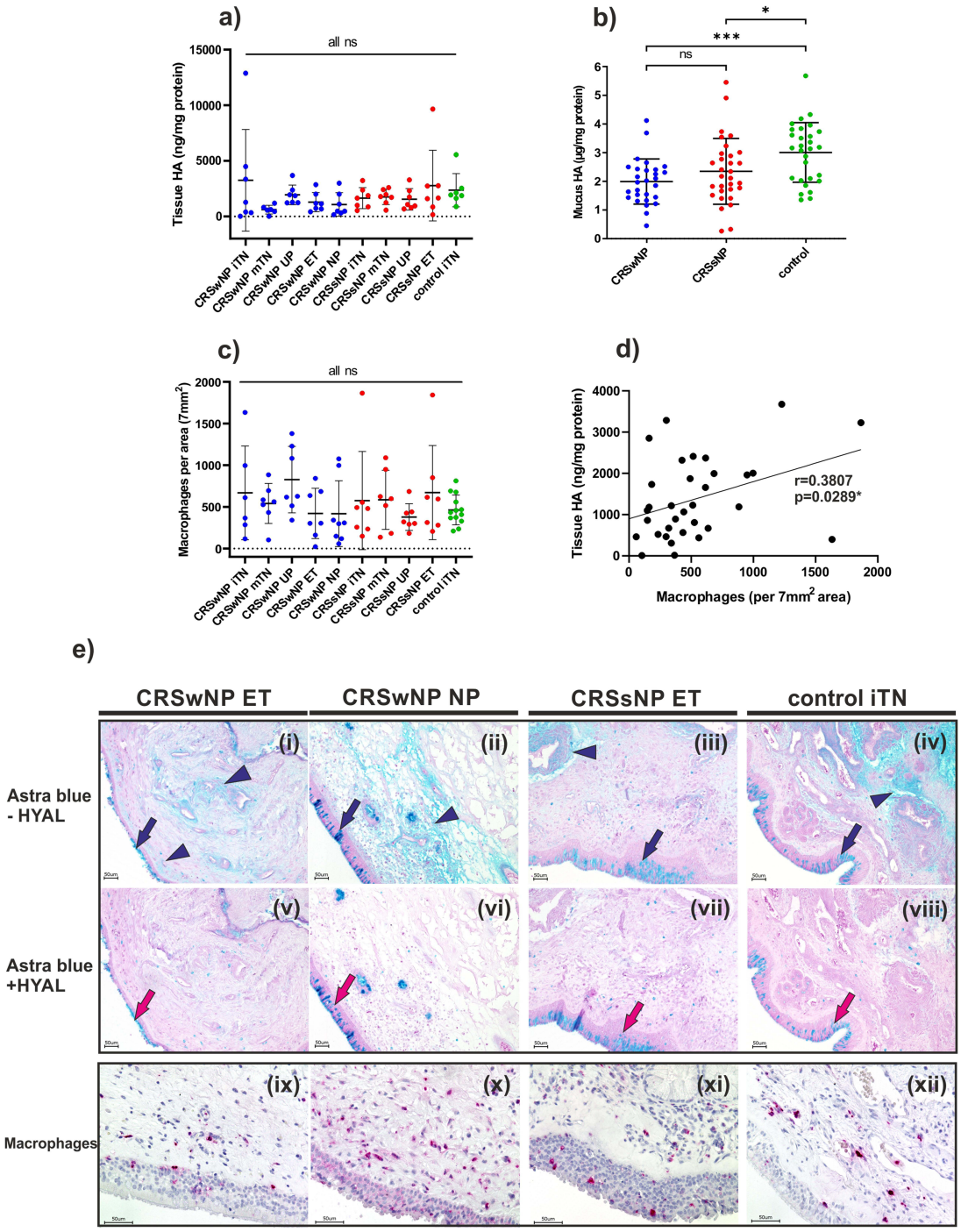

Figure 5 The scatter dot plot (**a**) including mean and SD error bars shows the non-significant results of the quantitative analysis of HA by ELISA in the tissue lysates (1 value below detection limit) of CRSwNP (blue), CRSsNP (red), and control (green) patients normalized to a total protein concentration. The scatter dot plot (**b**) including mean and SD error bars shows the results of the quantitative analysis of HA by ELISA in the nasal mucus (1 outlier, no value below detection limit) of CRSwNP (blue), CRSsNP (red), and control (green) patients normalized to a total protein concentration. Outliers are not included. Statistically significant differences can be seen for CRSwNP vs controls ($p<0.001$) and for CRSsNP vs controls ($p<0.05$). The scatter dot plot (**c**) including mean and SD error bars shows the non-significant results of the macrophage cell count in the tissue slides of CRSwNP (blue), CRSsNP (red), and control (green) patients normalized to an area of 7 mm^2. The scatter dot plot (**d**) shows the result of the correlation between HA and macrophages in nasal tissues. Immunohistochemistry (**e**) of HA (photographed with a 20x objective lens) and macrophages (photographed with a 40x objective lens) in CRSwNP, CRSsNP, and control tissues. Staining by Astra blue without degradation of HA by hyaluronidase is displayed in the panels (i), (ii), (iii) and (iv), whereas the panels (v), (vi), (vii) and (viii) show the same tissues after degradation of HA by hyaluronidase. Counterstaining was performed with Nuclear Fast Red. HA was found in both the epithelium (blue arrows) and the stroma (blue arrowheads). The outer epithelium additionally shows staining of mucopolysaccharides other than HA (pink arrows). Staining of macrophages is displayed in the panels (ix), (x), (xi) and (xii). Antigens were stained with Red Alkaline Phosphatase-Substrate, and counterstaining was performed with Harris' hematoxylin solution. Asterisks indicate statistically significant results. *<0.05, ***<0.001.

Abbreviations: CRSwNP, chronic rhinosinusitis with nasal polyps; CRSsNP, chronic rhinosinusitis without nasal polyps; iTN, inferior turbinate; mTN, middle turbinate; UP, uncinate process; ET, ethmoid; NP, nasal polyp; HA, hyaluronic acid; HABP, hyaluronic acid binding protein; HYAL, hyaluronidase; ns, not significant; SD, standard deviation.

Discussion

The aim of our study was to identify novel aspects that may be involved in the pathogenesis of CRS and especially polyp development and that may represent new targets for medical therapies. In addition, we wanted to know whether these factors differ between certain anatomical regions of the nasal mucosa and could thus be related to the likelihood of developing inflammation and NPs.

The staining of LVs in nasal tissues revealed that the wider LYVE-1$^-$/PDPN$^+$ (pre-)collector vessels were mainly located near the epithelium of the tissue sections, while the narrow LYVE-1$^+$/PDPN$^+$ LCs were mainly located in the inner stroma. Thus, we hypothesize that deeper tissue layers might be cleared more effectively than the outer layers. The counting of LVs revealed that CRSsNP iTN contained less of both LV types than the iTN of CRSwNP and the controls. Interestingly, the number of both LV types in all grouped CRSwNP and CRSsNP tissues were significantly lower than in the control iTN. Whereas inflammation generally induces lymphangiogenesis,[3] these findings suggest poor lymphangiogenesis in CRS-affected tissues. Respectively, a physiologically lower density of LVs in nasal tissues could favor the development of CRS. Probably the CRSwNP iTN was not affected by CRS, so that these circumstances do not apply with regard to this tissue. We hypothesize that in CRS the clearing of cell debris and interstitial water by lymphatics, and thus the healing process, is insufficient, supporting persistence and chronification.[3] Currently, the generally accepted theory regarding polyp formation is an excessive fibrin deposition induced by coagulation factor XIII-A. Simultaneously, the type 2 cytokines interleukin (IL)-4 and IL-13 suppress expression of the tissue plasminogen activator (t-PA), which would usually counteract the formation of a fibrin scaffold.[36] Since LC ends also act as liquid absorbers, they may be overwhelmed by the excessive amount of interstitial water leaking from hyperpermeable blood vessels during inflammation,[1,37] enabling the fibrin clot to further attract fluid.[36] This supports the result of a previous study which found that a lower LV density was associated with a higher risk of polyp formation.[17]

In order to examine levels of the lymphatic marker protein LYVE-1[1] in CRS, we performed ELISAs using the tissue lysates and nasal mucus of CRSwNP, CRSsNP, and controls. ELISA analysis of LYVE-1 in nasal tissues revealed the highest expression in NP and a continuous rise in LYVE-1 levels between the CRSwNP tissues mTN<UP<ET<NP, while comparison of the same tissue types in CRSsNP was not significant and did not differ from the control iTN. However, this result did not match the number of LYVE-1$^+$ lymphatic capillaries identified in the tissues. We assume that LYVE-1 detected by ELISA was mainly sLYVE-1, which is known to be generated by cleavage of the extracellular N-terminus by MMP-14.[5,6]

In order to examine the nasal mucosa for its main site of MMP-14 overexpression, we performed ELISAs using the tissue lysates of CRSwNP, CRSsNP, and controls. The results revealed a significant overexpression of MMP-14 in CRSwNP UP compared to CRSwNP iTN and control iTN. Interestingly, although levels of MMP-14 did not significantly differ between CRSsNP tissues, CRSsNP UP also showed a higher MMP-14 content compared to the other CRSsNP tissues. Given the fact that the uncinate process serves as a protective shield to prevent non-sterile inhaled air from reaching the sinuses,[38] the overproduction of proteases might be a defense mechanism against the absorbed harmful stimuli.[13] As a membrane-bound proteinase, MMP-14 was previously shown to cleave the ectodomain of LYVE-1 under pathological conditions including chronic inflammation. Proteolytic cleavage of LYVE-1 from the LCs consequently suppresses the production of vascular endothelial growth factor (VEGF)-C counteracting pathological LV growth.[5,6] Hence, we hypothesize that the cleaved sLYVE-1 is likely to ascend from the UP tissues of CRS patients, apparently diffuses through the mucosa, and ultimately accumulates in NP tissue. Moreover, an insufficient excretion due to fewer glands in CRSwNP tissues[39] or a compensatory mechanism to equalize LYVE-1 tissue content in NPs lacking LCs could further favorize this process. In the ELISA of mucus samples, LYVE-1 was significantly underexpressed in CRSsNP compared to CRSwNP and controls, which could be a consequence of an increased internalization of the protein into the LECs stimulated by tumor necrosis factor TNF-α,[40] that is known to be overexpressed in CRSsNP.

HA is a large glycosaminoglycan mainly located in the ECM where it acts as a stabilizer, hydrator, and regulator of wound healing.[7] For synthesis, three HA synthases located on the inner surface of the plasma membrane generate polymers of distinct sizes and extrude the nascent HA chains to the cell surface. HA metabolism varies depending on the situation. Normally, HA is initially degraded by hyaluronidases, cleaving it to products of intermediate sizes. These products are either degraded in lysosomes by local immune cells and ECM cells or enter LVs via LYVE-1, followed by terminal degradation in dLNs. An inflammatory state further increases HA turnover due to the increased activity of hyaluronidases, resulting in low molecular

weight (LMWHA) fragments that trigger immune responses as damage-associated molecular patterns (DAMPS).[1,7,41] However, since HA is capable of absorbing water equivalent to many times its own mass,[1] a high presence in polypus tissues supporting fluid retention would be imaginable.

In contrast to our expectations and consistent with a previous study,[42] the ELISA results of HA in different nasal tissues of CRSwNP, CRSsNP, and control patients did not show any significant differences. However, HA-staining showed that in NP tissue HA was concentrated within and below the epithelial layer, which was not the case in CRSsNP and control tissues, where HA was mainly located in the inner stroma. In the CRSwNP ET, an incipient rearrangement of the HA was evident. Other groups also localized HA around basal epithelial cells and in the basement membrane of NPs.[43] Therefore, we hypothesize that HA metabolism in NPs may be altered, triggering an accumulation of the HA at certain localizations of the nasal mucosa retaining liquid. In the ELISA of mucus samples, HA was significantly decreased in CRSwNP and CRSsNP compared to the controls. HA was proven to be secreted by respiratory epithelial cells and submucosal glands and to co-regulate mucociliary clearance that increases with smaller HA fragments.[44] Our results of HA in nasal secretion indicate that CRS may be associated with a reduced concentration of HA, which normally protects the nasal mucosa from harmful environmental influences.[44] Whether this is a trigger or a consequence of the CRS disease will need further investigation. The low HA content in CRSwNP mucus could also be due to the fact that CRSwNP tissues contain fewer glands[39] containing HA, which was shown by IHC. Still, our results support the outcomes of clinical trials where local HA administration via nebulized nasal douche or nasal spray reduced CRS symptoms.[44,45]

During the inflammatory state HA supports the motility, proliferation and activation of immune cells including macrophages.[7,9,10,46] The gathering of immune cells at the site of injury is important for proper healing processes.[47] However, for the following resolution of the inflammation and regeneration of the tissue, these cells should be cleared from the tissue by LVs.[3] The staining of macrophages in sections of the different tissue types confirmed other findings that these cells are particularly localized in the outer stroma, the basement membrane, the lamina propria, and the epithelium.[48] Probably, due to reduced cell density caused by HA accumulation and insufficient uptake by LVs, the immune cells are able to migrate more easily in these areas of the tissues, which may enable their gathering. While previous studies found macrophages to be particularly accumulated in NP tissue,[36] counting of macrophages revealed no significant differences either between the phenotypes or between the tissue types. However, in most CRS tissues there was a much higher variance compared to the control. Low immune cell counts in NP could be due to the generally low cell density in swollen tissue, where infiltrating factors can consequently spread more widely than in all other nasal tissues where the cell density is comparable. Another possible reason could be an inhomogeneous infiltration of the NP by macrophages, so that these were not present in some sections analyzed.

The correlation analysis between HA and macrophages in nasal tissues revealed a weakly significant positive correlation, supporting previous findings of HA attracting macrophages.[9,10]

The disruption of adherens junctions caused a by loss of E-cadherin and β-catenin was previously identified as the reason for enhanced cell migration within HA accumulation sites. Loose cell connections consequently facilitate cell motility and ECM remodeling, which in turn are favorable factors for the development of many diseases.[11,12,46,49]

In conclusion, our findings suggest that the lymphatics play an important role in CRS pathophysiology by causing a deviant distribution of hyaluronan and macrophages and thus supporting fluid retention and chronification of the disease.

Despite promising results there were some limitations to our study. Firstly, despite careful selection of the samples, additional factors other than CRS affecting the outcome cannot be completely ruled out. Secondly, the sample sizes per tissue type were relatively small. Thirdly, iTN served as our only control tissue. Especially since it has been described before that LVs physiologically occur with varying densities in different anatomical subsites,[50] the differences between the control iTN and the tissues of anatomical subsites other than iTN in CRS patients could therefore theoretically be physiological.

Since not much is known about the pathophysiological relationships between LVs and CRS to date, more studies will be needed in the future. Larger cohorts and different types of control tissues should be used to clarify our findings. The connections between the LVs and other inflammatory and pathogenic CRS factors such as other immune cells, fibrinogen and collagen,[13] should be investigated.

Overall, our study elucidates a novel and promising approach to explain the pathophysiology of CRS by analyzing the role of the lymphatic system. This warrants further analysis in the future to enable the exact connections with other pathways in CRS to be understood.

Conclusion

Lymphatic vessels and hyaluronan and may play essential roles in the pathogenesis of CRS via retention of fluid and macrophages. Inadequate lymphatic clearance may support the deposition of HA and immune cells and thus perpetuate the disease. These results may provide a novel approach to the identification of disease-associated factors.

Data Sharing Statement

The data that support the findings of this study are available from the corresponding author, upon reasonable request.

Ethical Approval

Ethical approval to report this case was obtained from institutional review board of the University of Erlangen-Nürnberg (No.: 17-269_1-B) on 11.02.2020. All participants provided written informed consent prior to participating.

We confirm that your study complies with the Declaration of Helsinki.

Acknowledgments

Thanks to Renate Schäfer[1] and Elisabeth Sterna[1] for methodical support.

Funding

This study was funded by the Else-Kröner-Fresenius Stiftung (2019_A119). The sponsor had no involvement from study design to submission of the paper for publication.

Disclosure

Ms Vanessa-Vivien Pesold reports that this paper was written within a PhD work that is financially supported by Else Kröner-Fresenius-Stiftung (EKFS), during the conduct of the study. Dr Sarina Mueller reports grants from Else-Kröner-Fresenius Stiftung, during the conduct of the study. The authors report no other conflicts of interest in this work. This article was performed in partial fulfillment of the requirements for obtaining the degree „Dr. rer. biol. hum.“at the FAU.

References

1. Johnson LA, Jackson DG. Hyaluronan and Its Receptors: key Mediators of Immune Cell Entry and Trafficking in the Lymphatic System. *Cells*. 2021;10(8):2061. doi:10.3390/cells10082061
2. Liu J, Yu C. Lymphangiogenesis and Lymphatic Barrier Dysfunction in Renal Fibrosis. *Int J Mol Sci*. 2022;23(13):56.
3. Schwager S, Detmar M. Inflammation and Lymphatic Function. *Front Immunol*. 2019;10:308. doi:10.3389/fimmu.2019.00308
4. Weber E, Aglianò M, Bertelli E, Gabriele G, Gennaro P, Barone V. Lymphatic Collecting Vessels in Health and Disease: a Review of Histopathological Modifications in Lymphedema. *Lymphat Res Biol*. 2022;20(5):468–477. doi:10.1089/lrb.2021.0090
5. Nishida-Fukuda H, Araki R, Shudou M, et al. Ectodomain Shedding of Lymphatic Vessel Endothelial Hyaluronan Receptor 1 (LYVE-1) Is Induced by Vascular Endothelial Growth Factor A (VEGF-A). *J Biol Chem*. 2016;291(20):10490–10500. doi:10.1074/jbc.M115.683201
6. Wong HL, Jin G, Cao R, Zhang S, Cao Y, Zhou Z. MT1-MMP sheds LYVE-1 on lymphatic endothelial cells and suppresses VEGF-C production to inhibit lymphangiogenesis. *Nat Commun*. 2016;7:10824. doi:10.1038/ncomms10824
7. Abatangelo G, Vindigni V, Avruscio G, Pandis L, Brun P. Hyaluronic Acid: redefining Its Role. *Cells*. 2020;9(7):1743. doi:10.3390/cells9071743
8. Jackson DG. Hyaluronan in the lymphatics: the key role of the hyaluronan receptor LYVE-1 in leucocyte trafficking. *Matrix Biol*. 2019;78-79:219–235. doi:10.1016/j.matbio.2018.02.001
9. Johnson P, Arif AA, Lee-Sayer SSM, Dong Y. Hyaluronan and Its Interactions With Immune Cells in the Healthy and Inflamed Lung. *Front Immunol*. 2018;9:2787. doi:10.3389/fimmu.2018.02787
10. Savani RC, Hou G, Liu P, et al. A role for hyaluronan in macrophage accumulation and collagen deposition after bleomycin-induced lung injury. *Am J Respir Cell Mol Biol*. 2000;23(4):475–484. doi:10.1165/ajrcmb.23.4.3944
11. Kultti A, Zhao C, Singha NC, et al. Accumulation of extracellular hyaluronan by hyaluronan synthase 3 promotes tumor growth and modulates the pancreatic cancer microenvironment. *Biomed Res Int*. 2014;2014:817613. doi:10.1155/2014/817613
12. Tahkola K, Ahtiainen M, Mecklin JP, et al. Stromal hyaluronan accumulation is associated with low immune response and poor prognosis in pancreatic cancer. *Sci Rep*. 2021;11(1):12216. doi:10.1038/s41598-021-91796-x
13. Fokkens WJ, Lund VJ, Hopkins C, et al. European Position Paper on Rhinosinusitis and Nasal Polyps 2020. *Rhinology*. 2020;58(Suppl S29).

14. Hao D, Wu Y, Li P, et al. An Integrated Analysis of Inflammatory Endotypes and Clinical Characteristics in Chronic Rhinosinusitis with Nasal Polyps. *J Inflamm Res*. 2022;15:5557–5565. doi:10.2147/JIR.S377301
15. Tomassen P, Vandeplas G, Van Zele T, et al. Inflammatory endotypes of chronic rhinosinusitis based on cluster analysis of biomarkers. *J Allergy Clin Immunol*. 2016;137(5):1449–56.e4. doi:10.1016/j.jaci.2015.12.1324
16. Cui N, Zhu X, Zhao C, Meng C, Sha J, Zhu D. A Decade of Pathogenesis Advances in Non-Type 2 Inflammatory Endotypes in Chronic Rhinosinusitis: 2012-2022. *Int Arch Allergy Immunol*. 2023;1–17.
17. Luukkainen A, Seppälä M, Renkonen J, et al. Low lymphatic vessel density associates with chronic rhinosinusitis with nasal polyps. *Rhinology*. 2017;55(2):181–191. doi:10.4193/Rhin16.007
18. Keck T, Lindemann J. Numerical simulation and nasal air-conditioning. *GMS Curr Top Otorhinolaryngol Head Neck Surg*. 2010;9:Doc08. doi:10.3205/cto000072
19. Kim DK, Eun KM, Kim MK, et al. Comparison Between Signature Cytokines of Nasal Tissues in Subtypes of Chronic Rhinosinusitis. *Allergy Asthma Immunol Res*. 2019;11(2):201–211. doi:10.4168/aair.2019.11.2.201
20. Peng Y, Zi XX, Tian TF, et al. Whole-transcriptome sequencing reveals heightened inflammation and defective host defence responses in chronic rhinosinusitis with nasal polyps. *Eur Respir J*. 2019;54(5):1900732. doi:10.1183/13993003.00732-2019
21. Tan BK, Klingler AI, Poposki JA, et al. Heterogeneous inflammatory patterns in chronic rhinosinusitis without nasal polyps in Chicago, Illinois. *J Allergy Clin Immunol*. 2017;139(2):699–703.e7. doi:10.1016/j.jaci.2016.06.063
22. Orlandi RR, Kingdom TT, Smith TL, et al. International consensus statement on allergy and rhinology: rhinosinusitis 2021. *Int Forum Allergy Rhinol*. 2021;11(3):213–739. doi:10.1002/alr.22741
23. Hardison SA, Senior BA. The argument against the use of dupilumab in patients with limited polyp burden in chronic rhinosinusitis with nasal polyposis (CRSwNP). *J Otolaryngol Head Neck Surg*. 2023;52(1):64. doi:10.1186/s40463-023-00668-z
24. Volmer T, Effenberger T, Trautner C, Buhl R. Consequences of long-term oral corticosteroid therapy and its side-effects in severe asthma in adults: a focused review of the impact data in the literature. *Eur Respir J*. 2018;52(4):1800703. doi:10.1183/13993003.00703-2018
25. Mueller SK, Wendler O, Nocera A, et al. Escalation in mucus cystatin 2, pappalysin-A, and periostin levels over time predict need for recurrent surgery in chronic rhinosinusitis with nasal polyps. *Int Forum Allergy Rhinol*. 2019;9(10):1212–1219. doi:10.1002/alr.22407
26. Selvarani R, Van Michelle Nguyen H, Thadathil N, et al. Characterization of novel mouse models to study the role of necroptosis in aging and age-related diseases. *Geroscience*. 2023;45(6):3241–3256. doi:10.1007/s11357-023-00955-7
27. Grigorev IP, Korzhevskii DE. Modern Imaging Technologies of Mast Cells for Biology and Medicine (Review). *Sovrem Tekhnologii Med*. 2021;13(4):93–107. doi:10.17691/stm2021.13.4.10
28. de la Motte CA, Drazba JA. Viewing hyaluronan: imaging contributes to imagining new roles for this amazing matrix polymer. *J Histochem Cytochem*. 2011;59(3):252–257. doi:10.1369/0022155410397760
29. Cold Spring Harbor Laboratory. Mowiol-DABCO stock solution. *Cold Spring Harb Protoc*. 2007.
30. Cardiff RD, Miller CH, Munn RJ. Manual hematoxylin and eosin staining of mouse tissue sections. *Cold Spring Harb Protoc*. 2014;2014(6):655–658. doi:10.1101/pdb.prot073411
31. Schneider CA, Rasband WS, Eliceiri KW. NIH Image to ImageJ: 25 years of image analysis. *Nat Methods*. 2012;9(7):671–675. doi:10.1038/nmeth.2089
32. Akishima Y, Ito K, Zhang L, et al. Immunohistochemical detection of human small lymphatic vessels under normal and pathological conditions using the LYVE-1 antibody. *Virchows Arch*. 2004;444(2):153–157. doi:10.1007/s00428-003-0950-8
33. Hirakawa S, Hong YK, Harvey N, et al. Identification of vascular lineage-specific genes by transcriptional profiling of isolated blood vascular and lymphatic endothelial cells. *Am J Pathol*. 2003;162(2):575–586. doi:10.1016/S0002-9440(10)63851-5
34. Quintanilla M, Montero-Montero L, Renart J, Martín-Villar E. Podoplanin in Inflammation and Cancer. *Int J Mol Sci*. 2019;20(3):707. doi:10.3390/ijms20030707
35. Tadeo I, Gamero-Sandemetrio E, Berbegall AP, et al. Lymph microvascularization as a prognostic indicator in neuroblastoma. *Oncotarget*. 2018;9(40):26157–26170. doi:10.18632/oncotarget.25457
36. Kato A. Immunopathology of chronic rhinosinusitis. *Allergol Int*. 2015;64(2):121–130. doi:10.1016/j.alit.2014.12.006
37. Medzhitov R. The spectrum of inflammatory responses. *Science*. 2021;374(6571):1070–1075. doi:10.1126/science.abi5200
38. Güngör G, Okur N, Okur E. Uncinate Process Variations and Their Relationship with Ostiomeatal Complex: a Pictorial Essay of Multidedector Computed Tomography (MDCT) Findings. *Pol J Radiol*. 2016;81:173–180. doi:10.12659/PJR.895885
39. Huang Y, Wang M, Hong Y, et al. Reduced Expression of Antimicrobial Protein Secretory Leukoprotease Inhibitor and Clusterin in Chronic Rhinosinusitis with Nasal Polyps. *J Immunol Res*. 2021;2021:1057186. doi:10.1155/2021/1057186
40. Johnson LA, Prevo R, Clasper S, Jackson DG. Inflammation-induced uptake and degradation of the lymphatic endothelial hyaluronan receptor LYVE-1. *J Biol Chem*. 2007;282(46):33671–33680. doi:10.1074/jbc.M702889200
41. Jackson DG. Immunological functions of hyaluronan and its receptors in the lymphatics. *Immunol Rev*. 2009;230(1):216–231. doi:10.1111/j.1600-065X.2009.00803.x
42. Rudack C, Prehm P, Stoll W, Maune S. Extracellular matrix components in nasal polyposis. *Acta Otolaryngol*. 2003;123(5):643–647. doi:10.1080/0001648021000028133
43. Laurent C, Yoon YJ, Hvidsten I, Hellström S. Hyaluronan and alpha-atrial natriuretic polypeptide in human nasal polyps: contributing factors to oedema formation and polyp growth? *Acta Otolaryngol*. 2003;123(3):406–412. doi:10.1080/0036554021000028123
44. Cassandro E, Chiarella G, Cavaliere M, et al. Hyaluronan in the Treatment of Chronic Rhinosinusitis with Nasal Polyposis. *Indian J Otolaryngol Head Neck Surg*. 2015;67(3):299–307. doi:10.1007/s12070-014-0766-7
45. Abbate V, Iaconetta G, Maglitto F, et al. A Comparative Study of Different Administrations of Nebulized Hyaluronic Acid After Endoscopic Endonasal Surgery for Chronic Rhinosinusitis. *Indian J Otolaryngol Head Neck Surg*. 2022;74(Suppl 2):1037–1043. doi:10.1007/s12070-020-02110-6
46. Kobayashi T, Chanmee T, Itano N. Hyaluronan: metabolism and Function. *Biomolecules*. 2020;10(11):1525. doi:10.3390/biom10111525
47. Chen L, Deng H, Cui H, et al. Inflammatory responses and inflammation-associated diseases in organs. *Oncotarget*. 2018;9(6):7204–7218. doi:10.18632/oncotarget.23208

48. Bernstein JM, Gorfien J, Noble B, Yankaskas JR. Nasal polyposis: immunohistochemistry and bioelectrical findings (a hypothesis for the development of nasal polyps). *J Allergy Clin Immunol*. 1997;99(2):165–175. doi:10.1016/S0091-6749(97)70091-5
49. Donelan W, Dominguez-Gutierrez PR, Kusmartsev S. Deregulated hyaluronan metabolism in the tumor microenvironment drives cancer inflammation and tumor-associated immune suppression. *Front Immunol*. 2022;13:971278. doi:10.3389/fimmu.2022.971278
50. Beule AG. Physiology and pathophysiology of respiratory mucosa of the nose and the paranasal sinuses. *GMS Curr Top Otorhinolaryngol Head Neck Surg*. 2010;9:Doc07. doi:10.3205/cto000071